Synthesis, Characterization, and Structural Investigations of Poly(ethyl acrylate)-*l*-polyisobutylene Bicomponent Conetwork

Béla Iván,*,† Kristoffer Almdal,*,‡ Kell Mortensen,‡ Ib Johannsen,‡ and Jørgen Kops§

Department of Polymer Chemistry and Material Science, Institute of Chemistry, Chemical Research Center, Hungarian Academy of Sciences, H-1525 Budapest, Pusztaszeri u. 59-67, P.O. Box 17, Hungary; The Danish Polymer Centre, Risø National Laboratory, DK-4000 Roskilde, Denmark; and The Danish Polymer Centre, Department of Chemical Engineering, Technical University of Denmark, Building 229, DK-2800 Lyngby, Denmark

Received January 14, 2000

ABSTRACT: A new bicomponent conetwork, poly(ethyl acrylate)-*linked*-polyisobutylene (PEtA-*l*-PIB), was synthesized by radical copolymerization of equal amounts of telechelic α,ω-dimethacrylic PIB (MA−PIB−MA, M_n/(kg/mol) = 11.2, M_w/M_n = 1.12, and MA/chain = 2.0) obtained via quasi-living carbocationic polymerization and ethyl acrylate in 10% solution for each component in a common solvent, tetrahydrofuran, followed by extraction and drying. Low amounts of extractables (2.5% in acetone and 4.6% in hexane) and nearly theoretical composition (51% PEtA and 49% PIB) of the resulting conetwork indicate efficient network formation; i.e., this new conetwork is composed of PIB chains connected at each end to two PEtA chains. DSC experiments gave close to literature value T_g's (−68 °C for PIB and −22 °C for PEtA), indicating a segregated morphology in this conetwork. In contrast to reported results for similar conetworks containing PIB and other polymers with polar groups, surface analysis with XPS found no significant difference in surface and bulk compositions in PEtA-*l*-PIB. For the first time in the field of bicomponent segmented conetworks, the structure of a conetwork was investigated by small-angle neutron scattering (SANS) in both the relaxed and strained states. Two correlation peaks were observed at q^*/Å^{-1} = 0.035 and at $3q^*$. The measured value of q^* is less by more than a factor of 2 than that predicted by de Gennes for random bicomponent ("grafted") networks. The macroscopically homogeneous conetwork is characterized by nanoscale local layered like segregation with a correlation length of 445 Å and periodicity of 180 Å. This structure does not deform affinely with the macroscopic deformation. The measured modulus is in excellent agreement with an affine network prediction assuming that each MA−PIB−MA chain gives rise to three elastic strands in the network.

Introduction

There has been significant interest in well-defined polymeric architectures in recent years. Polymers composed of segmented blocks have received much attention from both a scientific and a technological point of view. These materials can be applied not only as commodities, e.g., thermoplastic elastomers, but also as new nanostructured systems for a variety of new applications, such as biomaterials, high-tech devices, nanofabricated components, etc. (see, e.g., refs 1). Hence, synthesis of new polymeric materials consisting of segmented polymer blocks and understanding their structure, morphology, and properties are of increasing importance.

The synthesis of polymers consisting of segmented blocks has been mainly carried out via quasi-living polymerizations[2] by various mechanisms, such as carbocationic,[3,4] anionic,[5] free radical,[6] group transfer,[7] ring-opening metathesis,[8] and ring-opening polymerizations.[9] These processes have undergone rapid development during the past several years. The advances in this research field have led to a variety of new polymers with narrow molar mass distribution and most importantly with precise microstructures, such as macromonomers, telechelics, macrocycles, stars, blocks, and macromolecules with pendant functionalities. Exact telechelic macromolecules are of great interest as building blocks of bi- and multicomponent polymer architectures.[10,11] Telechelic polyisobutylenes (PIB) have attracted significant attention due to the advantageous properties including chemical, oxidative, thermal, and radiation stability of this polymer chain.[3,4]

One of the most interesting recent applications of telechelic PIBs is synthesis of bicomponent segmented conetworks in which the different block segments are covalently bonded to each other.[12−17] Several classes of new bicomponent polymer conetworks consisting of incompatible polymer chains, especially amphiphilic conetworks,[12−18] have recently received significant attention in both academia and industry for several potential new applications, e.g., biomaterials, contact lenses, implants, controlled drug delivery matrices, membranes, etc. However, the synthetic aspects, structure, and especially morphology of these new materials have not been fully revealed and understood yet. Most of the previous works in this field have concerned achieving attractive properties such as strength combined with the ability to swell in water and hydrophobic solvents through the combination of hydrophilic and hydrophobic parts of the conetwork. In this study we focus on the more fundamental aspects of bicomponent conetworks such as local structure, ordering phenomena, and the mechanical properties in the rubbery state. Thus, we have chosen two incompatible hydrophobic polymers with glass transitions temperatures, T_g's, below room temperature in order to facilitate such a study. This study concerns the synthesis, characterization, and small-angle neutron scattering (SANS) investigations of a new bicomponent conetwork, poly(ethyl acrylate)-*l*-polyisobutylene (PEtA-*l*-PIB) (*l* stands for *linked*; see refs 13 and 14 for definition).

† Hungarian Academy of Sciences.
‡ Risø National Laboratory.
§ Technical University of Denmark.
* Corresponding authors.

10.1021/ma000062+ CCC: $20.00
Published on Web 02/10/2001

Experimental Section

Materials. Solvents, such as dichloromethane, hexane, acetone, and tetrahydrofuran (THF), were purified by a conventional distillation procedure. Isobutylene (IB) (Hydro Gas Danmark, 99.8%) was passed through a drying column (Labclear gas filter, Aldrich) before condensation. Ethyl acrylate (Aldrich, 99%) and methacryloyl chloride (Aldrich, tech. 90%) were distilled under reduced pressure prior to use. Allyltrimethylsilane (ATMS, 99%), *N*,*N*-dimethylacetamide (DMA, anhydrous, 99.8%), and 0.5 M 9-borabicyclo[3.3.1]-nonane (9-BBN) in THF and $TiCl_4$ (99.9%) (all from Aldrich) were used as received. 1,3-Di(2-chloro-2-propyl)-5-*tert*-butylbenzene (tBuDiCumCl) was prepared as described earlier.[19] 2,2′-Azobis(isobutyronitrile) (AIBN) (Aldrich) was crystallized from methanol.

Synthesis of Methacrylate−Telechelic Polyisobutylene (MA−PIB−MA). Quasi-living carbocationic polymerization of isobutylene was carried out by the tBuDiCumCl/$TiCl_4$ initiating system in the presence of DMA in dichloromethane/hexane (40:60 v/v) solvent mixture at −78 °C using a simple laboratory process.[20,21] The concentration of tBuDiCumCl was 10^{-2} M, and the tBuDiCumCl/$TiCl_4$/DMA/IB molar ratio was 1:16:1:200. The polymerization was quenched with 2-fold excess of prechilled ATMS, resulting in exact allyl−telechelic polyisobutylene (PIB).[22,23] The allyl groups were transformed to primary hydroxyl termini by hydroboration with 9-BBN followed by oxidation as described elsewhere.[22−24] Finally, the hydroxyl-ended PIB was quantitatively esterified with methacryloyl chloride according to a literature procedure.[25] The resulting MA−PIB−MA was analyzed by SEC (M_n/(kg/mol) = 11.2, M_w/M_n = 1.12) and by ^{1}H NMR for end group functionality (F_n = 2.0).

Preparation of Poly(ethyl acrylate)-*l*-polyisobutylene (PEtA-*l*-PIB) Conetwork. Free radical copolymerization of ethyl acrylate (EtA) and MA−PIB−MA initiated by AIBN was carried out in THF solution containing 10% of EtA and the telechelic macromonomer in 1:1 weight ratio. A specially designed Teflon mold with 15 × 10 × 2 cm inner dimension was used for this reaction. After charging 4.8 g of EtA (4.8×10^{-2} mol) and 4.8 g of MA−PIB−MA (4.3×10^{-4} mol) in 48 mL of THF containing AIBN ($c_{AIBN}/M = 9.4 \times 10^{-4}$) under nitrogen, the mold was closed and placed in an oven having constant temperature of 60 °C for 72 h. Then THF was slowly evaporated from the resulting gel at room temperature. The sample was extracted with acetone until constant mass of the combined extractables was reached. Then the conetwork was dried to constant mass in vacuo at room temperature. Subsequently, it was extracted with hexane, and after reaching constant mass of the combined extractable material, the resulting conetwork was dried to constant mass in vacuo at ambient temperature.

Characterization. The composition of the PEtA-*l*-PIB conetwork was determined to be 49% by mass PIB by elemental analysis. Found: C, 72.5%; H, 11.1%; O, 16.4%.

Size exclusion chromatography (SEC) measurements were carried out at room temperature with a Nucleosil column set consisting of three columns (250 mm × 8 mm): 500 Å, 7 μ C_4; 100 Å, 5 μ C_8; and 50 Å, 5 μ C_3. THF was used as eluent with 1 mL/min elution rate. A dual RI and viscosity detector (Viscotek Co.) provided detection. Molar mass averages and molar mass distributions (MMD) were calculated by calibration with polystyrene standards (Polymers Laboratories).

A Perkin-Elmer Pyris 1 differential scanning calorimeter was used for differential scanning calorimetry (DSC). Carefully weighed samples in sealed aluminum pans were cooled to 153 K and analyzed in a heating, a cooling, and a second heating cycle between 153 and 453 K using a scan rate of 20 K/min.

The surface elemental composition of the polymer conetwork was analyzed by X-ray photoelectron spectroscopy (XPS) using a Specs SAGE 100 spectrometer. The photoelectrons were analyzed with a 30°, 45°, 60°, and 90° takeoff angle. For quantification, survey scans were combined with multiple scans of narrow energy regions using low pass energy.

Scheme 1. Formation of Poly(ethyl acrylate)-*l*-polyisobutylene Conetwork (PEtA-*l*-PIB)

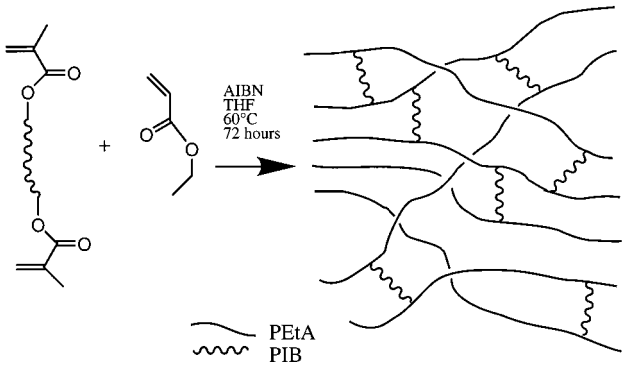

Small-Angle Neutron Scattering (SANS). Small-angle neutron scattering was performed on a ∼1 mm thick cast film of the PEtA-*l*-PIB sample. The scattering length densities of pristine PIB and PEtA are quite different, providing natural contrast for neutron scattering in these materials. The sample area was defined by an 8 mm diameter circular pinhole. The scattering experiments were obtained at the SANS facility at the cold source of the DR3 research reactor at Risø, Denmark. Two instrumental settings were used. In both cases the neutron wavelength was 5.6 Å, the wavelength-spread was 9%, and collimation length was 3 m. The one setting had the sample-to-detector distance of 1 m, while the other setting had 3 m. The raw data were corrected for incoherent background and detector sensitivity using the spectrum of water as a homogeneous scatterer. The incoherent scattering from water was used to estimate the incoherent background from the hydrogens in the sample, partly using the measured transmission factors. However, there might still be a minor contribution from incoherent scattering left in the data shown.

Combined SANS and Mechanical Extension Measurements. Simultaneous neutron scattering and mechanical testing data were obtained by mounting a sample of 12.0 × 0.65 mm^2 cross section in the film/fiber fixture of a Rheometrics RSA2 dynamical mechanical spectrometer. As the sample is a soft rubber, some degree of slippage in the tool cannot be ruled out. The sample length was 19.0 mm. The RSA2 has been custom modified to be mounted in the beam of the SANS instrument.[26] The spectra were azimuthally averaged over an 8 pixel narrow band parallel and perpendicular to the direction of stretching. No background correction was performed for the anisotropic scattering patterns.

Results and Discussion

A. Synthesis of MA−PIB−MA and PEtA-*l*-PIB Conetwork. The poly(ethyl methacrylate)-*l*-polyisobutylene (PEtA-*l*-PIB) conetwork was prepared by radical copolymerization of ethyl acrylate and methacrylate−telechelic polyisobutylene (MA−PIB−MA) as shown in Scheme 1. The exact telechelic MA−PIB−MA bifunctional macromonomer was obtained by quasi-living carbocationic polymerization of isobutylene followed by quenching with allyltrimethylsilane.[22,23] Further quantitative derivatizations, i.e., preparation of hydroxy−telechelic PIB, hydroboration/oxidation of the allyl termini,[22−24] and subsequent esterification of the hydroxyl termini with methacryloyl chloride,[25] led to MA−PIB−MA. The resulting polymer was analyzed by SEC and ^{1}H NMR. These analyses indicated that the desired exact methacrylate−telechelic PIB with average functionality of two (F_n = 2.0) and with predetermined molar mass and narrow molar mass distribution (M_n/(kg/mol) = 11.2 and M_w/M_n = 1.12) was obtained.

The MA−PIB−MA bismacromonomer acts as crosslinking agent during polymerization of ethyl acrylate,

leading to the PEtA-*l*-PIB conetwork. Three major requirements[12−14] should be met for the successful synthesis of such conetworks: (i) the bismacromonomer should copolymerize with the low molar mass comonomer; (ii) the length of the polymer chain formed from the low molar mass monomer should be sufficiently high in order to incorporate at least one bismacromonomer in order to reach the onset of network formation; (iii) phase separation between the components of the polymerization system should be prevented during copolymerization.

In relation to the first criterion the copolymerization reactivity ratios gives hints on the copolymerization process between the low molar mass monomer, ethyl acrylate in this case, and the methacrylate terminated bismacromonomer. However, copolymerization reactivity ratios for copolymerizations involving macromonomers are scarce in the literature. As well documented in recent studies[27,28] for the free radical copolymerization of *n*-butyl acrylate and methyl methacrylate, respectively, with methacrylate-ended poly(methyl methacrylate) macromonomers, the widely known Jaacks[29] method is applicable at high monomer feed ratios (56 in our case), i.e., the probability of propagation by reacting macromonomer with a macromonomer ended propagating chain is negligibly low, and thus r_2 should not be considered in such copolymerizations. In other words, the determining factor in the conetwork formation is the relative reactivity of the telechelic macromonomer toward the propagating chain ends containing the low molar mass monomer. Usually the low molar mass analogue of the polymerizing end group is taken into consideration first, i.e., methyl methacrylate for the MA−PIB−MA. The reactivity ratio r_1 for free radical copolymerization of ethyl acrylate (EtA) (M_1) and methyl methacrylate (MMA) (M_2) is between 0.22 and 0.47 according to literature data.[30] This means that the macroradicals with ethyl acrylate terminal unit preferentially react with MMA. In respect to the macromonomer this may result in the preferential incorporation of the bismacromonomer cross-linker in the growing chain. The apparent relative reactivity of macromonomers in free radical copolymerizations depends on the viscosity of the reaction medium, i.e., on the concentration and/or the chain length of macromonomers,[27,28] and therefore their reactivity is usually lower than that of the corresponding low molar mass monomer, MMA in our case. Therefore, we assume that in the case of copolymerization of EtA and a methacrylate-ended macromonomer the reactivity ratio is much closer to one than that for the low molar mass monomers, EtA and MMA. This situation may allow the efficient formation of poly(ethyl acrylate)-*l*-polyisobutylene conetworks with closely random distribution of the bismacromonomer MA−PIB−MA cross-linker along the PEtA chain. If the reactivity ratio was in the opposite direction, i.e., when $r_1 > 1$, formation of a large fraction of homopolymer and branched structures with the low extent of macromonomer incorporation could be expected.

As for the second requirement, the length of polymer chains can be controlled by the initiator/monomer ratio in free radical polymerizations. Usually $1/DP_n \sim [I]^{0.5}/[M]$ where DP_n is the number-average degree of polymerization, and [I] and [M] are the concentrations of initiator and monomer, respectively. Since [M] is given in most of the experiments, using low enough initiator concentration is the determining factor for obtaining long enough chains required for conetwork formation.

The most problematic aspect of the synthesis of conetworks between incompatible chain segments is prevention of phase separation during the synthetic process. This third and most critical requirement can be solved in two ways. The most obvious one is the preparation of the conetwork in a common solvent at sufficiently high temperature to provide a homogeneous one-phase system. Even in such cases phase separation may occur above certain critical composition, which leads to a limit in the variation of the composition of the conetworks.[31] The second successful approach uses polar monomers with selected nonpolar protecting groups for copolymerization with nonpolar telechelic macromonomers, and the protecting groups are removed in the resulting gel in order to obtain the desired conetwork with covalently bonded chain segments.[12,13,16]

Considering these requirements, the PEtA-*l*-PIB conetwork was prepared by the copolymerization of 50/50 w/w ethyl acrylate and MA−PIB−MA in THF solution at 60 °C for 3 days. The resulting material was dried and carefully extracted with acetone, a solvent for PEtA and the unreacted monomer, and subsequently with hexane, a solvent for PIB. Low amounts of extractables, 2.5% in acetone and 4.6% in hexane, were obtained, indicating highly efficient conetwork formation. Elemental analysis gave the mass fraction of PEtA and PIB in the extracted dry conetwork to be 0.51 and 0.49, respectively. These data also show that this process led to a conetwork with nearly quantitative incorporation of the components with the designed composition.

B. Surface Analysis of PEtA-*l*-PIB. Analysis of surface composition was carried out by XPS. PIB-based amphiphilic conetworks[15] and polyurethanes[32] with polar components contain higher amounts of nonpolar PIB in the surface layer than that measured in the bulk samples. This phenomenon is attributed to the low surface energy of PIB. Therefore, it was studied whether this is a general phenomenon with materials composed of nonpolar PIB and polymers with polar groups. XPS experiments found that the surface layer contains 81.2 ± 4.7 at. % carbon and 11.3 ± 3.1 at. % oxygen or 87.8 ± 3.4 at. % carbon and 12.2 ± 3.4 at. % oxygen disregarding the small amounts of other elements—silicon and fluorine—present in the surface. Assuming the fluorine and silicon to be due to poly(tetrafluoroethylene) (PTFE) and poly(dimethylsiloxane) impurities from the sample preparation (the sample was polymerized in an PTFE mold and handled between PTFE sheets), one can correct the surface composition to contaminant-free conditions. This procedure yields 90.1 ± 2.8 at. % carbon 9.9 ± 2.8 at. % oxygen. There is no systematic trends in the data as a function of takeoff angle of the photoelectrons (probing depth) or variation in sample treatment. The bulk composition is 85.5 at. % carbon and 14.5 at. % oxygen, which is slightly but not significantly lower than measured surface composition. In conclusion, the XPS data indicate that the bulk and surface composition of the PEtA-*l*-PIB conetwork are identical within experimental error. In comparison with earlier findings,[15] this exceptional result may require further systematic studies.

C. DSC Investigation. DSC can in many cases detect compositional heterogeneity, here PIB and PEtA rich domain formation. Figure 1 shows the DSC curve of PEtA-*l*-PIB. As presented in this figure, two glass transition temperatures (T_g) are observed: at −68 °C for PIB and at −22 °C for PEtA. These nearly literature values of the T_g's clearly indicate the existence of two incompatible domains in this conetwork.

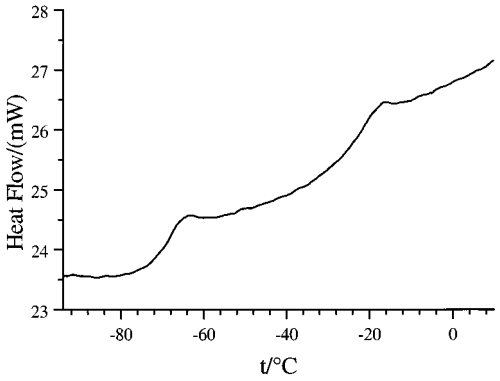

Figure 1. DSC scan with a heating rate of 20 °C/min for the PEtA-*l*-PIB network.

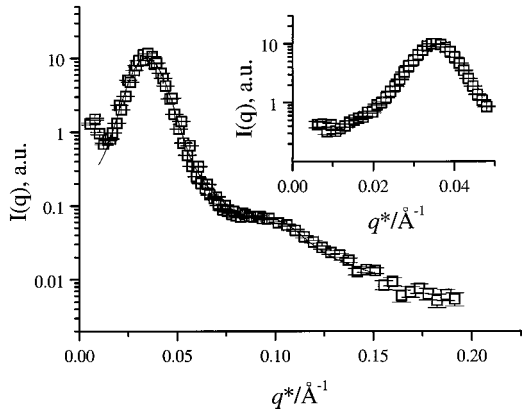

Figure 2. Isotropic SANS. Azimuthally averaged data combined from two detector distances (3 and 1.5 m) at 25 °C. The line is a fit to two Lorenztians. The inset shows data collected at 6 m detector distances at 30 °C.

D. Small-Angle Neutron Scattering. SANS data over a wide range of scattering vectors are shown in Figure 2. The most distinct feature of the experimental scattering function is the correlation peak at $q^*/\text{Å}^{-1} = 0.035$. A correlation peak is expected in a network consisting of polymer blocks like the present system. A weak but distinctively higher order reflection at $3q^*$ is also seen. Furthermore, the inset of Figure 2 shows that very low intensity is observed at low q. A correlation length of 445 Å and a periodicity of 180 Å can be extracted from a fit (see below). These data indicate that the sample is macroscopically homogeneous. The conclusion is substantiated by the fact that the material is optically clear. Thus, no phase separation took place during the polymerization of PEtA. At a local scale a layered-like ordered structure exists with incompatible PEtA and PIB domains. However, the order is weak as seen from the close to equal size of the correlation length and the periodicity.

A somewhat more sophisticated analysis can be made on the basis of a theoretical study by de Gennes. Here the structure factor of a network made up of two polymers, which are cross-linked at random, but where only AB-type of cross-links are considered.[33] In this system, de Gennes showed that the scattering function approaches the form

$$S^{-1}(q) = Cq^{-2} + \frac{1}{2}(\chi_0 - \chi) + \frac{1}{24}b^2q^2 \qquad (1)$$

where C is a parameter related to the internal rigidity of the chain. C was estimated to be of the order of $C \approx 36/(n^2b^2)$, where n is the mean degree of polymerization between cross-links, b is the statistical segment length, χ is the Flory−Huggins segmental interaction parameter, and χ_0 is a critical value giving rise to some kind of microphase separation. The actual state beyond $\chi > \chi_0$ was not, however, resolved. According to eq 1, the scattering function of randomly cross-linked A and B polymers will show a peak at

$$q^* = 5.42/n^{1/2}b = 5.42/r_0^{1/2} \qquad (2)$$

where $r_0^{1/2}$ is the mean end-to-end distance of the chains between cross-links.

The PEtA-*l*-PIB conetwork deviates somewhat from the model that de Gennes was discussing in the sense that the network is not made up of randomly cross-linked polymers. On the contrary, all PIB segments interconnecting branching knots have a well-defined size with narrow molar mass distribution. The PEtA segments, on the other hand, have a molar mass distribution that is in principle unknown but that is anticipated to approach the most probable distribution. Only the mean value is known, since the overall volume fraction of PEtA is close to $f_{\text{PEtA}} = 0.5$; i.e., the average volume of PEtA is close to the well-defined volume of PIB segments. Overall, however, we do not expect that these deviations will cause major differences from the model discussed by de Gennes; only minor changes in prefactors can be expected, and these are only crudely estimated anyway. The mean distance between cross-links $\langle r_0^2\rangle$ can be estimated from literature values of $\langle r_0^2\rangle/M$. At 298 K $(\langle r_0^2\rangle/M)_{\text{PIB}}/(\text{Å}^2\text{mol g}^{-1}) = 0.570$[34] and $(\langle r_0^2\rangle/M_{\text{PEtA}})/(\text{Å}^2\text{mol g}^{-1}) = 0.522$.[35] With $\rho_{\text{PIB}}/(\text{g cm}^{-3}) = 0.918$ and $\rho_{\text{PEtA}}/(\text{g cm}^{-3}) = 1.12$[36] $\langle r_0^2\rangle/\text{Å}^2 = {}^2/_3 M_{\text{PIB}}/\rho_{\text{PIB}}\cdot(0.5(\langle r_0^2\rangle/M_{\text{PEtA}})\rho_{\text{PEtA}} + 0.5(\langle r_0^2\rangle/M_{\text{PIB}})\rho_{\text{PIB}}) = 4.5 \times 10^3$. We find according to eq 2 $q^* = 0.081$ Å^{-1}, significantly larger than the measured value of 0.035 Å^{-1}. The model[33] assumes that the conformation of the melt is unperturbed by the formation of the cross-links. The observed domain spacing is much larger than anticipated, indicating significant stretching of the coils similar to the situation in diblock copolymers.[37]

Briber and Bauer have previously investigated a somewhat related system.[38] They conducted SANS experiments on a radiation cross-linked polymer mixture of deuterated polystyrene, dPS, and poly(vinyl methyl ether), PVME, and also found scattering as described by eq 1. The q^* value of the dPS−PVME network appeared as in the present study to be smaller by a factor of 2 as compared to the theoretical expectations, assuming random cross-link density. The variation of q^* with dose, D, and thereby cross-link density, however, showed perfect linear $q^* \sim D^{1/2}$ behavior in agreement with simple calculations.

Already the publication by de Gennes[33] argued that the network might form segregated domains on the length scale of the mesh size, provided the χn value is sufficiently large. The observation of two distinct glass transitions in the PEtA-*l*-PIB conetwork confirms such segregation. The values of the two T_g's are close to those of the pure components, indicating that the material is in a type of strong segregation limit. The scattering patterns of the PEtA-*l*-PIB conetwork further confirm segregation by revealing an ordered structure on the mesoscopic length scale. Beyond the first-order peak at q^* already discussed, the scattering function shows a clear additional peak at $q = 3q^*$, in agreement with a lamellar ordered structure. The two peaks correspond

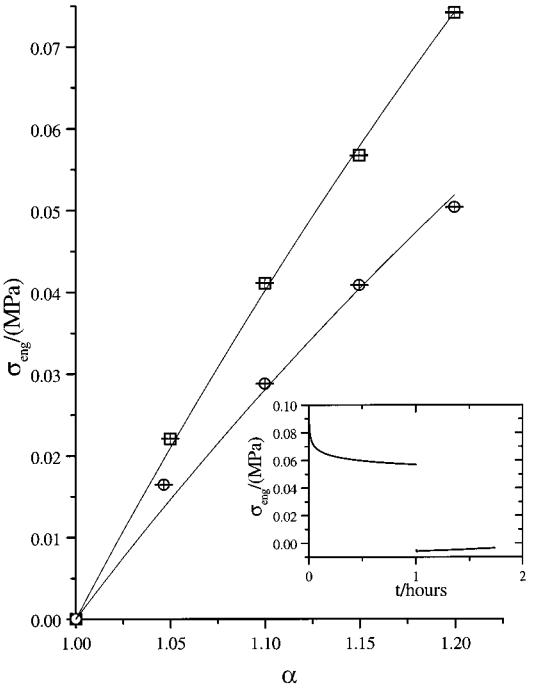

Figure 3. Engineering stress of the PEtA-*l*-PIB network as a function of elongation ratio at 25 °C (□) and 60 °C (○). The lines are fits and represent a Hookean solid (see text) with E/MPa = 0.441 ± 0.006 at 25 °C and E/MPa = 0.308 ± 0.006 at 60 °C, respectively. The inset shows data at 25 °C, α = 1.15. At t = 0 h α was changed from 1 to 1.15 in 10 s, and at t/hours = 1 α was changed from 1.15 to 1 in 10 s.

to the first- and third-order Bragg reflections, respectively. The absence of the second order is in agreement with the composition $f = 0.5$. Thus, like diblock copolymers, the segmented conetwork surprisingly also forms lamellar ordered mesophase near symmetric composition. The solid line in Figure 2 represents a best fit to two, instrument resolution broadened Lorentzian peaks.[39] The resulting parameters from this analysis give $q_{10} = 0.035$ Å^{-1}, corresponding to a lamellar periodicity of $d = 2\pi/q_{10} = 180$ Å. The ratio $q_{30}/q_{10} = 3$ as expected. The peak width gives the correlation length of $\xi = 440$ Å, i.e., only 2−3 lattice distances. The lamellar ordered structure is therefore incorporated with significant amounts of disorder, which may be both in the form of dislocations and as significant distribution in domain sizes. This is quite easy to understand, as the cross-linked nature prevents the system to optimize both the size and the form of the segregating domains.

E. Combined SANS Stretching Measurements. The network was stretched from the nonstrained state (extension ration α = 1) to the desired elongation in 10 s and kept at this elongation for 1 h while the force was measured and neutron scattering patterns were recorded. After the elapse of 1 h the extension ratio was set back to 1 during 10 s and the stress recorded for another 45 min. In none of the cases was a true equilibrium stress recorded, as is evident from the inset in Figure 3 where the data from one such experiment is given. The stress relaxes after the extension, and a compressive stress is observed when the extension is released. Both the extensional and compressive stress relax at a similar rate. The extension part of the stress curves could be fitted by the function $\sigma_{eng} = \sigma_0 + A_1 \exp(-t/\tau_1) + A_2 \exp(-t/\tau_2)$ where the amplitudes A_1 and A_2 were of similar magnitude; τ_1 and τ_2 were approximately 50 and 1000 s, respectively. The stress, σ_0, was taken to represent the equilibrium stresses of the network. Obviously the choice of two relaxation times is arbitrary, and a real possibility exists that the network can relax further at long relaxation times. However, the low amount of extractables indicates an efficient cross-linking, and it is speculated that the slow relaxation is due to reorganization of the microstructure rather than a loose network structure. The resulting equilibrium stresses of the network are given in Figure 3. The sample is assumed to behave as a Hookean solid, and the data are fit to the equation $\sigma_{eng} = (E/3)(\alpha - \alpha^{-2})$,[40] where σ_{eng} is the engineering stress and E is Young's modulus. Young's moduli of 0.44 MPa at 25 °C and 0.31 MPa at 60 °Care obtained. Note that these values must be regarded as having a relatively large uncertainty.

If one assumes perfect cross-linking and no influence of the microstructure on the modulus, one can estimate Young's modulus from the theory of rubber elasticity. Each bifunctional PIB chain is connected to four elastic active chains of PEtA. However, each PEtA chain is also connected to another PIB chain so that the number of elastic chains in the ideal case is 3 times the number of PIB chains. Then $E = 3((f-2)/f)\nu RT$, [41] where f is the functionality of the junction point (here 3), ν is the number density of elastic chains, and $\nu = 3w\rho/M_{n,PIB}$, where w is the mass fraction of PIB in the network. With $M_{n,PIB}$/(kg/mol) = 11.2 and the average density ρ/(g/cm^3) = 1.01, E/MPa = 0.32, which is surprisingly close to the measured modulus.

The effect of stretching on the microstructure of the PEtA-*l*-PIB network is qualitatively seen in Figure 4. The stretching is accompanied by a stretching of the microstructure parallel to the stretching direction—the scattering peak moves to smaller scattering vector—and a corresponding contraction perpendicular to the stretching direction—the scattering peak moves to larger scattering vector. The effect was quantified by analyzing the peak position parallel and perpendicular to the stretching direction. These peak positions were obtained by fitting a Gaussian to the data in the two directions. There is no relaxation in the position of the scattering peaks, and the data were analyzed by averaging the scattering over the entire period the sample was kept at one particular elongation (see Figure 7).

Figure 5 shows such data as a function of the extension ratio, α. Incompressibility requires that $\alpha_{||}\alpha_{\perp}^2 = 1$ where $\alpha_{||} \equiv \alpha$ is the deformation parallel to the stretching direction and $\alpha_{\perp}$ is the deformation perpendicular to the stretching direction. Thus, $\alpha_{\perp} = \alpha^{-1/2}$. The scattering peak position is a measure of the size of the domain structure in the sample, and thus the relative peak position perpendicular to the stretching direction $q^*_{\perp}(\alpha)/q^*(1)$ should scale as $\alpha^{1/2}$ if the domain size deformed affinely. Similarly, $q^*_{||}(\alpha)/q^*(1)$ should scale as α^{-1} in this case. The outer envelope of dotted lines in Figure 5 represent α^{-1} and $\alpha^{1/2}$. This is clearly not the case. The change in the domain size is much smaller. Another option is that the cross-linking point and thus the end-to-end distances of the chains deform affinely. The calculation in ref 33 is performed under a weak segregation limit assumption. From this assumption follows that the domain size scales as $D \sim r_0^{1/2}$ and thus $q^* \sim D^{-1} \sim r_0^{-1/2}$. If the chains deform affinely, then $r_0 \sim \alpha$ and $q^*_{||}(\alpha)/q^*(1) \sim r_{0,||}^{-1/2} \sim \alpha^{-1/2}$ and $q^*_{\perp}(\alpha)/q^*(1) \sim r_{0,\perp}^{1/2} \sim \alpha^{1/4}$, where $r_{0,||}$ and $r_{0,\perp}$ are the end-to-end distance of the chains parallel and perpendicular to the stretching direction, respectively. The inner envelope of

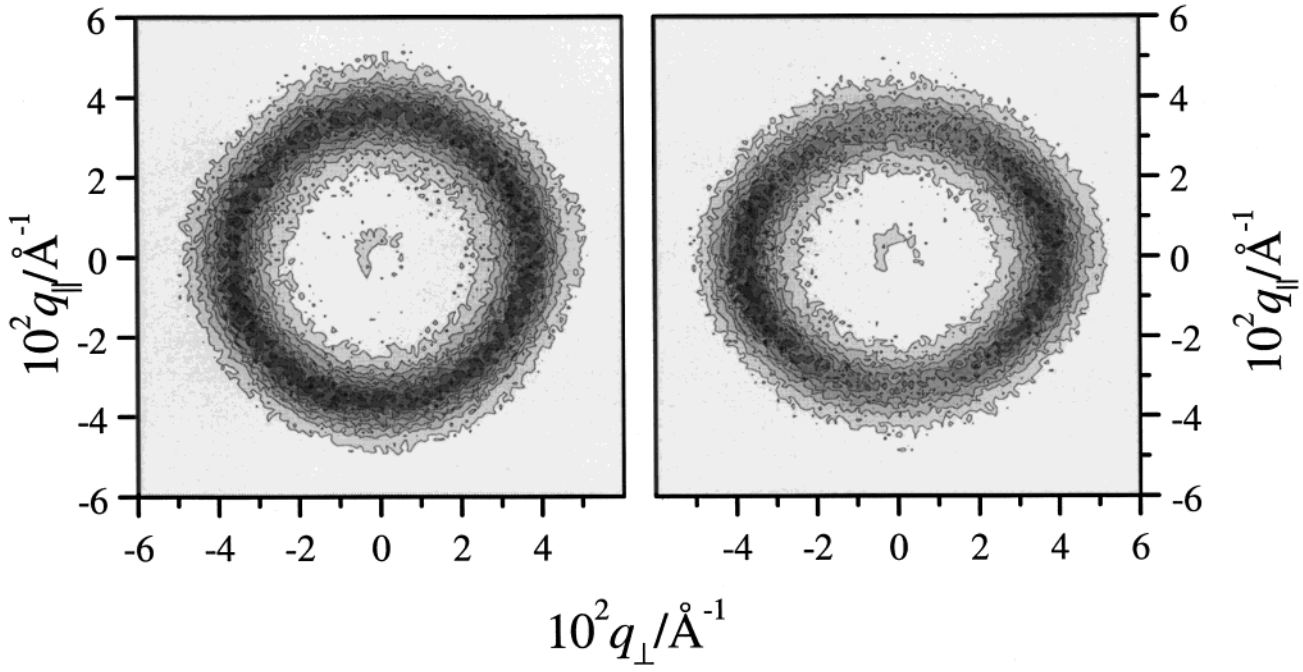

Figure 4. 2-D SANS data for the PEtA-*l*-PIB network at 60 °C for $\alpha = 1$ (left pattern) and $\alpha = 1.2$ (right pattern).

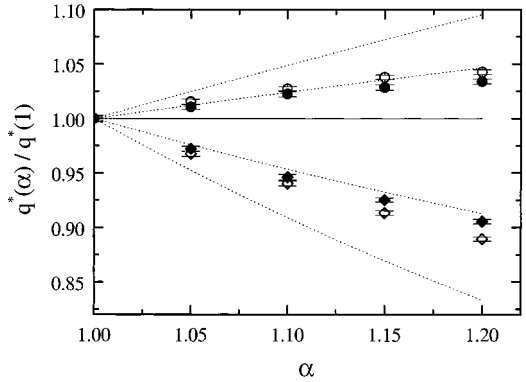

Figure 5. Ratio $q^*(\alpha)/q^*(1)$ of the scattering peak position at elongation ratio α to scattering peak position at $\alpha = 1$ as a function of α. Relative peak position perpendicular to the stretching direction $q^*_\perp(\alpha)/q^*(1)$ at 25 °C (○) and 60 °C (●). Relative peak position parallel to the stretching direction $q^*_\parallel(\alpha)/q^*(1)$ at 25 °C (◇) and 60 °C (◆). The dotted lines are guides to the eye for affine deformation of either the chain or the domain structure (see text) and represent α^{-1}, $\alpha^{-0.5}$, $\alpha^{0.25}$, and $\alpha^{0.5}$, respectively.

dotted lines in Figure 5 represents $\alpha^{-1/2}$ and $\alpha^{1/4}$. Figure 5 shows that the actual behavior is close to affine deformation of the chains. To quantify this, we present the same data in a different manner in Figure 6. The isotropic scattering pattern at $\alpha = 1$ (Figure 2) shows that the network is locally ordered. It is known from diblock copolymers that close to the order-to-disorder transition the scaling exponent, ν, of domain spacing with chain length, $D \sim n^\nu$, is significantly larger than the value $^1/_2$ that follows from the weak segregation assumption.[37] If this is incorporated in the scaling relations as $D \sim r_0^\nu$, then $q^*_\parallel(\alpha)/q^*(1) \sim r_{0,\parallel}^{-\nu} \sim \alpha^{-\nu}$ and $q^*_\perp(\alpha)/q^*(1) \sim r_{0,\perp}^{1/2} \sim \alpha^{\nu/2}$. These relations suggest plotting $-\ln(q^*_\parallel(\alpha)/q^*(1))$ vs $\ln(\alpha)$ and $2\ln(q^*_\perp(\alpha)/q^*(1))$ vs $\ln(\alpha)$. Figure 6 shows such plots. The peak positions follow a scaling law in the direction parallel to the stretching but not perpendicular to stretching. Furthermore, ν is neither 1 nor $^1/_2$ but a number in between and fairly close to $^1/_2$ at 60 °C. Figure 3 showed that

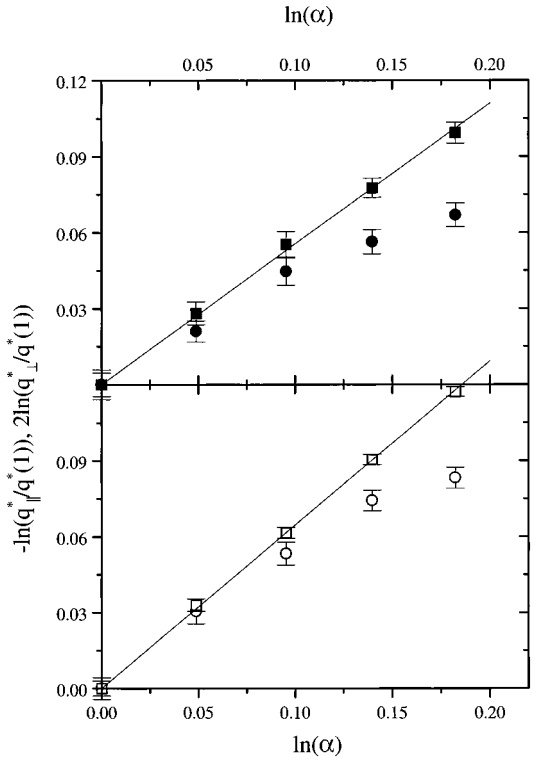

Figure 6. Scaling behavior of the relative peak scattering position parallel, $q^*_\parallel/q^*(1)$ (■, □), and perpendicular, $q^*_\perp/q^*(1)$ (●, ○), to the stretching direction at 60 °C (top) and 25 °C (bottom). The lines are fits through (0,0) to the data parallel to the stretching direction and have slopes of 0.555 ± 0.006 (60 °C) and 0.646 ± 0.003 (25 °C).

the mechanical stress did not relax completely to equilibrium during the 1 h period the sample was kept at each α. Thus, it is not possible to distinguish between dynamic and thermodynamic reasons for the decrease in the scaling parameter ν.

In Figure 7 $q^*_\parallel/q^*$ and $q^*_\perp/q^*$ at both 25 and 60 °C are shown as a function of time. Each point is the average of 10 min of counting time. Within the limited

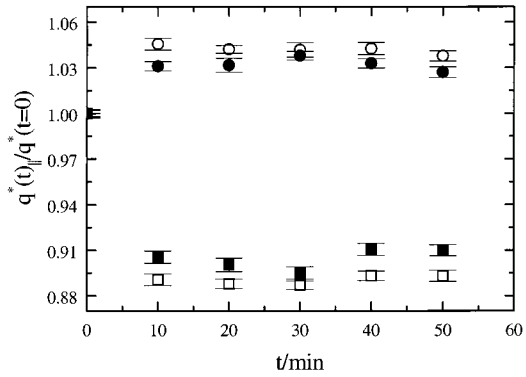

Figure 7. Evolution of the relative peak position $q^*_{\parallel}(t)/q^*(t = 0)$ at 25 °C (□) and 60 °C (■) and $q^*_{\perp}/q^*$ at 25 °C (○) and 60 °C (●) as a function of time after the stretching. $\alpha = 1.2$.

time resolution there is no clear tendency in the development of the scattering peak position, and thus q^* does not seem affected by the relaxation of the mechanical stress shown in Figures 3. Nonaffine deformation of the domains provides a plausible explanation of the relatively slow relaxation of the mechanical stress toward an equilibrium value after changes in the extension ratio.

Conclusion

A PEtA-*l*-PIB conetwork was successfully synthesized. DSC and SANS analysis indicates a locally segregated—ordered—structure of the network. Upon deformation, the end-to-end distances of the network chains deform nearly affinely whereas the domain structure undergoes reorganization.

Acknowledgment. This study was supported by the Danish Materials Technology Program MUP2, The Danish Technical Research Council & NATO (NATO funds, Grant 9800426), and was carried out within the framework of the Danish Polymer Centre.

References and Notes

(1) (a) Hillmyer, M. A.; Bates, F. S.; Ryan, A.; Fairclough, P.; Almdal, K.; Mortensen, K. *Science* **1996**, *271*, 976. (b) Stupp, S. I.; LeBonheur, V.; Walker, K.; Li, L. S.; Huggins, K.; Keser, M.; Amstutz, A. *Science* **1997**, *276*, 384. (c) Park, M.; Harrison, C.; Chaikin, P. M.; Register, R. A.; Adamson, D. H. *Science* **1997**, *276*, 1401. (d) Goldacker, T.; Abetz, V.; Stadler, R.; Erukhimovich, I.; Leibler, L. *Nature* **1999** *398*, 137. (e) Hadjichristidis, N. *J. Polym. Sci., Part A: Polym. Chem.* **1999**, *37*, 857 and references therein.

(2) (a) Iván, B. *Macromol. Symp.* **1994**, *88*, 201. (b) Iván, B. *Makromol. Chem, Macromol. Symp.* **1993**, *67*, 311.

(3) Kennedy, J. P.; Iván, B. *Designed Polymers by Carbocationic Macromolecular Engineering*: *Theory and Practice*; Hanser Publishers: Munich, 1992.

(4) Iván, B.; Kennedy, J. P. In *Macromolecular Design of Polymeric Materials*; Plast. Eng. Ser., Vol. 40; Hatada, K., Kitayama, T., Vogl, O., Eds.; Marcel Dekker: New York, 1997; p 51.

(5) Quirk, R. P.; Hsieh, L.-H. *Anionic Polymerization*; Marcel Dekker: New York, 1998.

(6) (a) Georges, M. K.; Veregin, R. P. N.; Kazmaier, P. M.; Hamer, G. K. *Macromolecules* **1993**, *26*, 2987. (b) Wang, J.-S.; Matyjaszewski, K. *J. Am. Chem. Soc.* **1995**, *117*, 5614. (c) Kato, M.; Kamigaito, M.; Sawamoto, M. *Macromolecules* **1995**, *28*, 1721.

(7) Hertler, W. R. In *Macromolecular Design of Polymeric Materials*; Plast. Eng. Ser., Vol. 40; Hatada, K., Kitayama, T., Vogl, O.; Eds.; Marcel Dekker: New York, 1997; p 109.

(8) Novak, B. M.; Risse, W.; Grubbs, R. H. *Adv. Polym. Sci.* **1992**, *102*, 47.

(9) Aida, T. *Prog. Polym. Sci.* **1994**, *19*, 469.

(10) Goethals, E. J., Ed.; *Telechelic Polymers*; CRC Press: Boca Raton, FL, 1989.

(11) Webster, O. W. *Science* **1991**, *251* 887.

(12) Iván, B.; Kennedy, J. P.; Mackey, P. W. U.S. Patent, 5,073,-381, Dec 17, 1991.

(13) (a) Iván, B.; Kennedy, J. P.; Mackey, P. W. *Polym. Prepr.* **1990**, *31* (2), 217. (b) Iván, B.; Kennedy, J. P.; Mackey, P. W. In *Polymeric Drugs and Drug Delivery Systems*; ACS Symp. Ser., Vol. 469; Dunn, R. L., Ottenbrite, R. M., Eds.; American Chemical Society: Washington, DC, 1991; p 203.

(14) (a) Iván, B.; Kennedy, J. P.; Mackey, P. W. *Polym. Prepr.* **1990**, *31* (2), 215. (b) Iván, B.; Kennedy, J. P.; Mackey, P. W. In *Polymeric Drugs and Drug Delivery Systems*; ACS Symp. Ser., Vol. 469; Dunn, R. L., Ottenbrite, R. M., Eds.; American Chemical Society: Washington, DC, 1991; p 194.

(15) Park, D.; Keszler, B.; Galiatsatos, V.; Kennedy, J. P.; Ratner, B. D. *Macromolecules* **1995**, *28*, 2595.

(16) Janecska, Á.; Iván, B. *Polym. Mater. Sci. Eng.* **1998**, *79*, 477.

(17) (a) Park, D.; Keszler, B.; Galiatsatos, V.; Kennedy, J. P. *J. Appl. Polym. Sci.* **1997**, *66*, 901. (b) Erdodi, G.; Iván, B. *Polym. Mater. Sci. Eng.* **1998**, *79*, 481.

(18) (a) De Clercq, R. R.; Goethals, E. J. *Macromolecules* **1992**, *25*, 1109. (b) Goethals, E. J.; De Clercq, R. R.; Walraedt, S. R. *J. Macromol. Sci., Pure Appl. Chem.* **1993**, *A30*, 679. (c) Du Prez, F. E.; Goethals, E. *Macromol. Chem. Phys.* **1995**, *196*, 903. (d) Du Prez, F. E.; Goethals, E. J.; Schué, R.; Quariouh, H.; Schué, F. *Polym. Int.* **1998**, *46*, 117. (e) Lai, Y.-C.; Valint, P. L., Jr. *Polym. Mater. Eng. Sci.* **1995**, *72*, 116. (f) Lai, Y.-C. *Polym. Mater. Eng. Sci.* **1995**, *72*, 118. (g) Künzler, J.; Ozark, R. *J. Appl. Polym. Sci.* **1995**, *55*, 611. (h) Delebra, M.; Ebdon, J. R.; Rimmer, S. *Macromol. Rapid Commun.* **1997**, *18*, 723.

(19) Wang, B.; Mishra, M. K.; Kennedy, J. P. *Polym. Bull.* **1987**, *17*, 205.

(20) Everland, H.; Kops, J.; Nielsen, A.; Iván, B. *Polym. Bull.* **1993**, *31*, 159.

(21) Feldthusen, J.; Iván, B.; Müller, A. H. E.; Kops, J. *Macromol. Rapid Commun.* **1997**, *18*, 417.

(22) Iván, B.; Kennedy, J. P. *Polym. Mater. Sci. Eng.* **1988**, *58*, 869.

(23) Iván, B.; Kennedy, J. P. *J. Polym. Sci, Part A: Chem. Ed.* **1990**, *28*, 89.

(24) Iván, B.; Kennedy, J. P.; Chang, V. S. C. *J. Polym. Sci., Polym. Chem. Ed.* **1980**, *18*, 3177.

(25) Kennedy, J. P.; Hiza, M. *J. Polym. Sci., Polym. Chem. Ed.* **1983**, *21*, 1033.

(26) Vigild, M. E.; Almdal, K.; Mortensen, K.; Hamley, I. W.; Fairclough, J. P. A.; Ryan, A. J. *Macromolecules* **1998**, *31*, 5702.

(27) Roos, A. S. G.; Müller, A. H. E.; Matyjaszewski, K. *Macromolecules* **1999**, *32*, 8331.

(28) Radke, W.; Müller, A. H. E. *Makromol. Chem., Macromol. Symp.* **1992**, *54/55*, 583.

(29) Jaacks, V. *Makromol. Chem.* **1972**, *161*, 161.

(30) (a) Grassie, N.; Torrance, B. J. D.; Fortune, J. D.; Gemmel, J. D. *Polymer* **1965**, *6*, 653. (b) Markert, G. *Makromol. Chem.* **1967**, *103*, 109. (c) Bevington, J. C.; Harris, D. O. *J. Polym. Sci.* **1967**, *B5*, 799.

(31) Weber, M.; Stadler, R. *Polymer* **1988**, *29*, 1071.

(32) Yoon, S. C.; Ratner, B. D.; Iván, B.; Kennedy, J. P. *Macromolecules* **1994**, *27*, 1548.

(33) de Gennes, P. G. *J. Phys., Lett.* **1979**, *40*, L69.

(34) Fetters, L. J.; Lohse, D. J.; Richter, D.; Witten, T. A.; Zirkel, A. *Macromolecules* **1994**, *27*, 4639.

(35) Penzel, E.; Goetz, N. *Angew. Makromol. Chem.* **1990**, *178*, 201.

(36) Van Krevelen, D. W. *Properties of Polymers. Their Correlation with Chemical Structure; Their Numerical Estimation and Prediction from Additive Group Contributions*, 3rd ed.; Elsevier: Amsterdam, 1990.

(37) Almdal, K.; Rosedale, J. H.; Bates, F. S.; Wignall, G. D.; Fredrickson, G. H. *Phys. Rev. Lett.* **1990**, *65*, 1112.

(38) Briber, R. M.; Bauer, B. J. *Macromolecules* **1988**, *21*, 3296.

(39) Pedersen, J. S.; Posselt, D.; Mortensen, K. *J. Appl. Crystallogr.* **1990**, *23*, 321.

(40) Macosko, C. W. *Rheology. Principles, Measurements, and Applications*; VCH Publishers. New York, 1994.

(41) Pearson, D. S.; Graessley, W. W. *Macromolecules* **1980**, *13*, 1001.

MA000062+